Computerized Atlas-Guided Positioning of Deep Brain Stimulators: A Feasibility Study

Benoit M. Dawant[1], Rui Li[1], Ebru Cetinkaya[1], C. Kao[2], J. Michael Fitzpatrick[1], and Peter E. Konrad[2]

[1] Department of Electrical Engineering and Computer Science, Vanderbilt University, Nashville, Tennessee
[2] Department of Neurological Surgery, Vanderbilt University, Nashville, Tennessee
Benoit.Dawant@vanderbilt.edu

Abstract. Optimal placement of a deep brain stimulator (DBS) is an iterative procedure. A target is chosen preoperatively based on anatomical landmarks identified on MR images. This point is used as an initial position that is refined intraoperatively using both micro-electrode recordings and macrostimulation. Because the length of the procedure increases with the time it takes to adjust the DBS to its final position, a good initial position is critical. In this work we explore the possibility of using an atlas and non-rigid registration algorithms to select the initial position automatically. We compare the initial DBS position obtained with this approach and the initial position selected by a neurosurgeon with the final position for eight STN (subthalamic nucleus) cases. Our results show that the automatic method leads to initial positions that are closer to the final positions than the initial positions selected manually.

1 Introduction

Since its first FDA approval in 1998 deep-brain stimulation (DBS) has gained significant popularity in the treatment of movement disorders [1,2]. The therapy has significant application in the treatment of tremor, rigidity, and drug induced side effects in patients with Parkinson's disease and essential tremor. The use of a 4-contact electrode, as shown in Figure 1 (Medtronic #3387or #3389 *quadripolar lead*®; Medtronic, Inc., Minneapolis, MN) placed within targets ranging from 4-12 mm in diameter requires stereotactic neurosurgical methodology. Ideally, the optimal target for therapy should be located within the stimulation range of 1 or 2 contacts, each contact measuring 1.5mm separated by either 1.5mm (lead #3387) or 0.5mm (lead #3389). Effective stimulation results when the contacts surround the target [3, 4]. At our institution, we prefer that 2 contacts lie above and 2 contacts lie below the target. If the contacts are located as little as 2mm away from the desired target, ineffective stimulation results due to several reasons: a) failure to capture control of the group of neurons, b) stimulation of non-desirable areas resulting in unpleasant stimulation, or c) necessity for higher stimulus intensities to produce the desired effect resulting in reduced battery life of the implant. For these reasons, targeting the specific neurons of interest for this therapy requires millimetric precision and allowance for variability among patients. Hence, the process of implantation of a DBS electrode follows from a

J.C. Gee et al. (Eds.): WBIR 2003, LNCS 2717, pp. 142 –150, 2003.

step-wise progression of a) initial estimation of target localization based on imaged anatomical landmarks, b) intraoperative micro-anatomical mapping of key features associated with the intended target of interest, c) adjustment of the final target of implantation by appropriate shifts in three-dimensional space, and d) implantation of the quadripolar electrode with contacts located surrounding the final desired target. In current clinical practice at our institution, the initial target localization is done manually on MR images based on AC-PC coordinates. In this work we present preliminary data that indicate that the initial target localization could be achieved automatically using non-rigid registration techniques. The data presented herein also indicate that initial target localization predicted by the automatic method is closer or as close to the optimal localization than the initial target localization chosen manually.

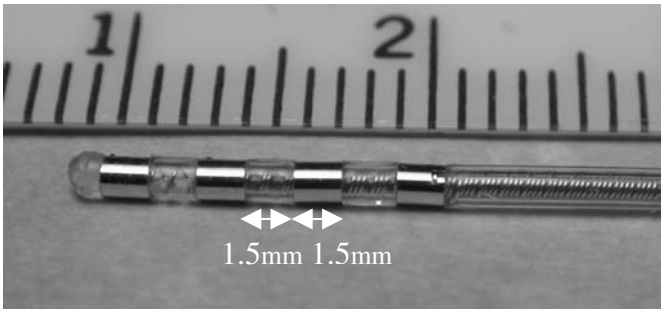

Fig. 1. Medtronic #3387 quadripolar lead® (Medtronic, Minneapolis, MN). Each silver band is one electrode. The numbers on the ruler indicate centimeters.

2 Material and Method

2.1 Patientsa and Preoperative Target Selection

All patients undergoing consideration for DBS implantation of the STN are first evaluated by a movement disorders neurologist and optimized on medications. If patients reach advanced parkinsonian symptoms (rigidity, bradykinesia, tremor, dyskinesias) despite optimal medical therapy, they are considered for surgical therapy by a multi-disciplinary group involving neurology, neurosurgery, neurophysiology, neuropsychiatry specialists. Target selection is decided upon by the team if no contraindications exist. A majority of patients with the above symptoms are recommended for STN targeting of DBS therapy. Target identification is performed by the functional neurosurgeon (PEK) and is based on an identification of the AC-PC location and arriving at 4mm posterior, 12mm lateral, and 4mm inferior to the midcommissural point for STN. Changes in the intended target are modified based on width of the third ventricle and other anatomical asymmetries noted on the MRI scan, but these adjustments usually only consist of less than 1mm deviations from the initial intended target location.

2.2 Guidance System and Surgical Procedure

Traditional methodology for carrying out this stepwise target localization and implantation procedure has been based on an externally fixed, rigid fixture, called a "stereotactic frame" that encompasses the patient's head and upon which the micromanipulating equipment can be mounted and maneuvered with sub-millimetric precision. These various stereotactic frames have been optimized to obtain accurate images used to create the initial target trajectory and plan and then to reduce erroneous movement associated with passage of the test electrodes and the final implant [5]. These frames typically require mounting the day of surgery, subsequent imaging with either CT and/or MRI axial slices, and target planning prior to starting the actual procedure of intraoperative mapping and ultimate placement of the electrode implant into the final target.

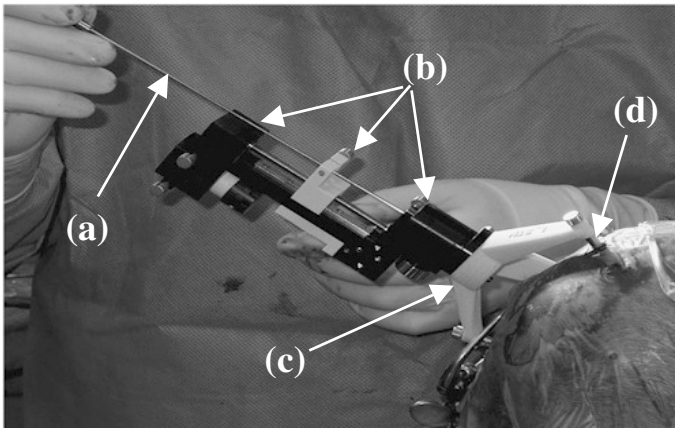

Fig. 2. Surgeon inserting probe (a) into micropositioning drive (b). The drive is attached to the Starfix platform (c). Each leg of the platform is mounted on one marker post, which is outfitted with an adaptor for this purpose (d).

Recently, a market-cleared and CE-compliant miniature stereotactic positioner called a *microTargeting Platform* became clinically available (*microTargeting Drive System for Stereotactic Positioning, incorporating STarFix guidance*, FHC Inc., Bowdoinham, Me.) This device, which we will call a platform, allows for more versatility with elective stereotactic procedures, such as DBS implantation. The platform is currently manufactured as a customized tripod that can be mounted on bone-based fiducial markers. Each platform is uniquely manufactured based on a stereotactically planned trajectory using software designed to mathematically relate the location of such bone markers with respect to brain structures [6]. The bone-based fiducial markers are of a two-piece design in which a fluid-filled cylinder that is visible on both CT and MR is detachably attached to a post that is implanted into the outer table of the skull. These images can then be used in the stereotactic software to designate a trajectory in relation to the bone-based marker posts. The plan is sent to the manufacturer who then translates the stereotactic plan into a customized platform for a given trajec-

tory through a rapid prototyping facility. The resultant platform is shipped to the hospital within 1 week and is used for mounting the same types of micromanipulators that are used on traditional stereotactic frames. The remaining portion of the procedure is the same with respect to intraoperative localization of the final target of implantation with the patient awake.

For each patient, the following data acquistion protocol and preoperative procedure is followed. First, under anesthesia the posts are implanted, Acustar™ (Z-Kat, Inc., Hollywood, FL) fiducial markers[1] are attached to the posts. The use of this marker and post in open craniotomies has been reported on earlier [6]. CT and MR volumes are acquired with the patient anesthetized and head taped to the table to minimize motion. (CT images acquired at kvp = 120V, exposure = 350mas, 512x512 pixels ranging in size from 0.49 to 0.62 mm, slice thickness = 2 mm for one patient, 1.3 mm for 2 patients, 1mm for all others; MR images are 3D SPGR volumes, TR: 12.2, TE: 2.4, voxel dimensions 0.85X0.85X1.3mm^3 except for subject 7 for which the voxel dimensions are 1X1X1.3mm^3). After imaging, the markers are removed. With the help of MR-CT registration software (VoXim^R, FHC, Inc.), the surgeon selects the initial target points based on AC-PC coordinates and associated entry points on the surface of the skull. In addition, the centroids of the markers and the directions of their posts are determined. These data are sent electronically to a fabrication plant where a customized platform is manufactured to fit the posts and provide an opening positioned over the entry point and oriented toward the target.

Surgery begins with the drilling of a burr hole (14 mm). An adaptor is attached to each post, the platforms are attached to the adaptors, and a micropositioning drive (microTargeting^R drive system, FHC Inc., Bowdoinham, ME) is attached to each platform (Figure 2). Micro-electrode recording leads are advanced into the patient to the respective initial target positions through the central tube guide of the platform. Resting firing frequencies are noted and the target positions are revised. The revision involves three-dimensional adjustment. In addition to changes in depth, it is possible to re-insert a probe along parallel tracks distributed within a 10 mm circle around the initial track. The microelectrodes are removed and a unipolar macrostimulation lead is inserted to the revised positions as determined by the micro-electrode recordings. With the patient awake, response to stimulation is monitored as the positions of the probes are further adjusted. When the final positions are selected, the DBS leads are inserted, buried beneath the scalp, and the platform is removed. During the entire procedure coordinates are read on the mircodrive. These physical coordinates can be transformed into preoperative CT coordinates using the software used for preoperative planing.

2.3 Automatic Atlas Creation

The atlas is a common frame of reference in which the position of each individual DBS can be recorded. This requires the spatial normalization of each individual brains. To do so we have used two algorithms developed at our institution. The first one is an independent implementation of the “demons” algorithm proposed by Thirion [8]. The second one is a new algorithm we have developed recently [9] that we call

[1] JMF is a consultant for, and has an interest in, Z-Kat, Inc., Hollywood, FL, which markets this marker.

the Adaptive Basis Algorithm (ABA). In this technique, inspired by the work of Rueckert *et al.* [10] and Meyer *et al* [11], the deformation that registers one image onto the other is modeled with a linear combination of radial basis functions with finite support. The similarity measure used to drive the registration process is the mutual information between the images. In this algorithm, several improvements over existing mutual information-based non-rigid registration algorithm are implemented. These include working on an irregular grid, adapting the compliance of the transformation locally, decoupling a very large optimization problem into several smaller ones, and deriving schemes to guarantee the topological correctness of the transformations. This algorithm computes the final transformation iteratively across scales and resolutions (in this context, resolution means the spatial resolution of the image while the scale is related to the transformation itself). A standard image pyramid is created to apply the algorithm at different resolutions. At each resolution, the scale of the transformation is adapted by modifying the region of support and the number of basis functions (the scale of the transformation is indeed related to the bases' region of support; a large region of support leads to a transformation at a large scale). Typically the algorithm is initialized on a low resolution image with few basis functions having large support. As the algorithm progresses to finer resolutions and smaller scales, the region of support of the basis functions is reduced. Following this approach, the final deformation field is computed as

$$\mathbf{v}(\mathbf{x}) = \mathbf{v}_1(\mathbf{x}) + \ldots + \mathbf{v}_M(\mathbf{x}).$$

with M the total number of levels with one level referring to a particular combination of scale and resolution. In this study we have chosen empirically one of the MR volumes as the atlas. All the other MR volumes are then registered automatically to the atlas using both algorithms. Once the transformation between one image volume and the atlas is computed, the spatial coordinates of the DBS in this volume can be transformed into atlas coordinates. The optimun DBS position in the atlas is computed as the centroid of all the DBS positions after their projection onto the atlas. But because the intraoperative coordinates are given in terms of preoperative CT coordinates and because the non-rigid registration algorithms need to be applied on MR images, an additional step is required. Corresponding MR and CT image volumes are registered using a rigid body transformation also computed using mutual information as proposed by Maes et al. [12].

2.4 Prediction of the Optimum Target Position with the Atlas

Predicting the DBS position for each patient is the inverse of the operation described above. It consists in projecting the optimum DBS position from the atlas to each individual image volume. This does not require another registration step because we compute the transformation from the patient to the atlas and from the atlas to the patient simultaneously. Our algorithms impose constraints on these transformations to keep them almost inverse of each other to produce bijective transformations.

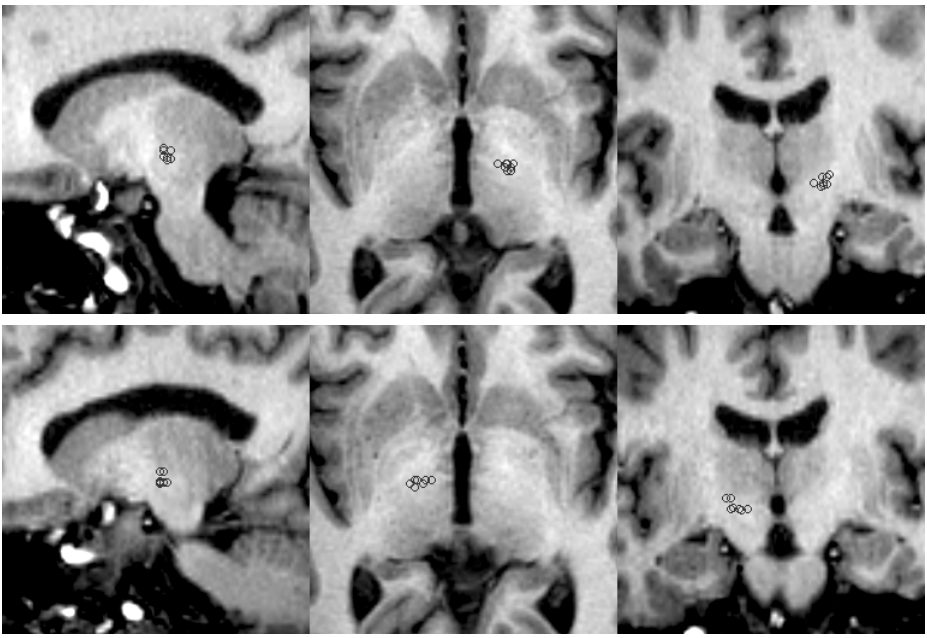

Fig. 3. Final location of the DBSs in the atlas projected onto the sagital, transverse, and coronal planes passing trough their centroid; top left side; bottom right side.

3 Results

3.1 Visual Evaluation of the Registration Results

Figure 3 shows the location of each of the DBSs in the atlas created with the ABA algorithm (results obtained with the demons algorithm are qualitatively similar). To generate these figures the position of these points has been projected on the sagital, transverse, and coronal planes passing through their centroid. The top panels show the left side, the bottom panels the right side.

3.2 Projection of the Final DBS Positions onto the Atlas

Tables 1 and 2 list the coordinates of the final DBS position transformed into atlas coordinates for eight bilateral STN patients using both algorithms. The centroid for the left and right sets of points has been computed. The Euclidean distance between each point and its corresponding centroid is reported in the Dc column. The distance between the left centroids computed with the ABA algorithm and the demons algorithm is 1.22mm. The distance between the right centroid computed with the ABA algorithm and the demons algorithm is 1.16mm. These results show that the final position of the DBSs transformed into atlas coordinates result in tight clusters. It is also worth noting that even though these two algorithms are based on very different

similarity measures (one minimizes the intensity difference between images on a voxel-by-voxel basis, the other maximized the Mutual Information between the volumes) they lead to essentially identical results.

Table 1. Position of the DBS position transformed into atlas coordinates using the ABA algorithm. Dc refers to distance from centroid

Adaptive Basis Algorithn								
	Left (all values are in mm)				*Right (all values are in mm)*			
	X	Y	Z	Dc	X	Y	Z	Dc
S1	124.28	106.39	53.98	***2.58***	95.47	106.20	53.20	*3.52*
S2	121.88	106.30	53.44	***1.44***				
S3	122.47	107.80	51.18	***1.43***	96.86	107.02	50.24	*2.12*
S4	119.79	106.27	51.78	***2.74***	101.38	104.91	50.23	*3.40*
S5	123.42	107.41	51.40	***1.42***	99.10	105.99	50.19	*1.35*
S6	123.42	107.99	53.21	***1.82***	96.68	104.69	52.96	*2.57*
S7	122.48	105.80	51.90	***1.07***	97.54	104.98	50.51	*0.92*
S8	121.70	106.60	50.91	***1.52***	99.85	104.69	49.63	*2.34*
Mean	*122.43*	*106.82*	*52.22*	*1.75*	*98.12*	*105.49*	*51.00*	*2.32*
STD	*1.37*	*0.81*	*1.16*	*0.60*	*2.07*	*0.91*	*1.45*	*0.97*

Table 2. Position of the DBS position transformed into atlas coordinates using the demons algorithm. Dc refers to distance from centroid.

Demons Algorithm								
	Left (all values are in mm)				*Right (all values are in mm)*			
	X	Y	Z	Dc	X	Y	Z	Dc
S1	124.28	106.39	53.98	*2.29*	95.47	106.20	53.20	*2.90*
S2	121.60	104.24	54.43	*1.94*				
S3	122.03	106.52	53.04	*0.88*	95.92	105.95	51.87	*2.14*
S4	120.31	106.73	51.97	*2.54*	99.78	105.72	51.23	*2.21*
S5	123.11	106.00	52.77	*1.08*	98.85	104.68	51.94	*1.08*
S6	122.42	105.63	54.60	*1.32*	97.01	103.79	53.97	*2.44*
S7	121.86	104.44	53.44	*1.32*	97.89	104.19	52.34	*0.89*
S8	122.07	105.63	52.16	*1.15*	99.92	104.58	49.61	*3.22*
Mean	*122.21*	*105.70*	*53.30*	*1.56*	*97.83*	*105.01*	*52.02*	*2.12*
STD	*1.15*	*0.93*	*0.99*	*0.61*	*1.78*	*0.94*	*1.40*	*0.87*

3.3 Comparison between Manually Selected and Atlas-Suggested Initial Target Positions

Table 3 presents the Euclidean distance computed between the final DBS position selected intraoperatively and (a) the initial position chosen manually and preoperatively by the neurosurgeon, (b) the initial position suggested by projecting the DBS position from the atlas onto each subject using the ABA algorithm and (c) the same as in (b) but with the demons algorithm.

Table 3. Distance between the initial position selected manually and automatically and the final position selected intraoperatively

Distances between original and final DBS position (in mm)							
	Left				***Right***		
Subject	Manual	ABA	Demons		Manual	ABA	Demons
S1	5.95	2.58	2.40		6.94	3.52	2.94
S2	5.72	1.78	3.39				
S3	2.53	2.41	1.50		4.49	2.45	2.23
S4	5.30	2.46	2.80		1.99	3.24	2.36
S5	2.31	2.17	1.00		3.64	1.60	1.51
S6	5.95	2.36	2.85		7.31	3.39	3.84
S7	2.00	1.64	2.37		2.01	1.75	1.68
S8	1.71	1.75	0.70		1.67	2.94	3.67
Mean	*3.93*	*2.14*	*2.13*		*4.01*	*2.70*	*2.60*
Std	*1.94*	*0.37*	*0.96*		*2.36*	*0.78*	*0.91*

4 Conclusions and Discussion

The results presented in this paper, albeit based on a small number of subjects, indicate that a fully automatic method for DBS target identification is possible. With both algorithms, the final position of the DBS, when mapped onto the atlas lead to tight clusters with average point-to-centroid distance in the order of 1.5 voxel. With both algorithms, the initial target points also are substantially closer to the final ones than the initial target point chosen manually (the average distance between initial and final position is 45% smaller with the automatic method on the left side and 30% on the right). Despite the small size of our data set the distance between the initial target points and the final target points is significantly smaller ($P<0.01$, one sided paired t-test) than the distance between the initial target points chosen manually and the final target points for both algorithms on the left side. On the right side, the significance drops to ($P<0.07$) and ($P<0.06$) for the ABA and the demons algorithms, respectively.

Atkinson et al. [13] have also explored the idea of using an atlas for movement disorder related surgery. This group correlated the clinical efficacy of stereotactic thalamotomy for tremor with anatomical localization by using postoperative magnetic resonance (MR) imaging and a deformable atlas of subcortical structures. These authors have been able to demonstrate a significant difference in the position of the lesion in their atlas for patients in three clinical outcome groups: excellent, good, and fair. However, they do not provide data in which the position of the lesion predicted by the atlas can be quantitatively compared to either the initial position selected by the neurosurgeon or the final position chosen intraoperatively. Other differences include the fact that their procedure is performed with a stereotactic frame and that they rely on a lesion to eliminate the tremor rather than an implantable stimulator.

A number of issues remain to be investigated. Because the number of patients for which we have the necessary data is limited, we have evaluated our approach on the set used to create our atlas. This may bias the results in our favor. As the number of data sets increase, we will separate the volumes into training and testing set to address

this issue. The best way to develop the atlas also remains an area of investigation. In the current study we have chosen one image volume as our atlas. We have not studied the impact of this choice on the results. We have also used all the image volumes we had at our disposal regardless of clinical outcome. A better approach may be to select only cases for which the clinical outcome is excellent to build the atlas.

If verified, the results presented herein may have a significant impact on the availability of the procedure. It is estimated that in the US alone 10-20,000 patients would benefit from DBS implantation each year. This number of procedures cannot be performed in leading research institution alone in which neurosurgeons have years of experience selecting targets manually. It is hoped that computer-assistance in target identification might make this procedure easier to perform by less experienced surgeons and hence make it available to many patients to whom it would otherwise remain inaccessible.

References

1. Referen G. Deuschl, J. Volkmann, P. Krack, "Deep brain stimulation for movement disorders", *Movement Disorders*, vol.17 (supplement 3) pp, S1-S1, 2002.
2. B. Schrader, W. Hamel, D. Weinert, H. M. Mehdorn, "Documentation of electrode localization.", *Movement Disorders*, vol. 17 (supplement 3), pp S167-S174, 2002.
3. Vitek, J.L., Mechanisms of deep brain stimulation: excitation or inhibition. *Mov Disord*, 2002. 17 Suppl 3: p. S69-72.
4. Lozano, A.M., Deep brain stimulation for Parkinson's disease. 2001. 7(3): p. 199-203.
5. R. L. Galloway and R. J. Maciunas, "Stereotactic neurosurgery", *Crit Rev Biomed Eng* 18(3), pp. 181-205, 1990.
6. J. Franck, P. Konrad, R. Franklin, F. Haer, D. Hawksley. "STarFix: A Novel Approach to Frameless Stereotactic Neurosurgery Utilizing a Miniaturized Customized Pretargeted Cranial Platform Fixture – Technical Description, Unique Features, and Case Reports", *Movement Disorders Society*, 7th Intl. Congress of Parkinsons Disease & Movement Disorder, Miami, FL, November 2002.
7. C. R. Maurer, Jr., J. M. Fitzpatrick, M. Y. Wang, R. L. Galloway, Jr., R. J. Maciunas, and G. S. Allen, "Registration of head volume images using implantable fiducial markers," *IEEE Trans. Med. Imaging,* vol. 16, pp. 447-462, 1997.
8. J.-P. Thirion, "Image matching as a diffusion process: an analogy with Maxwell's demons*". Medical Image Analysis*, vol. 2, no. 3, pp. 243-260, 1998.
9. G. Rhode, A. Aldroubi and B. M. Dawant, "The Adaptive-bases algorithm for intensity-based nonrigid image registration," *IEEE Transactions on Medical Imaging* (in press, 2003)
10. D. Rueckert, L. I. Sonoda, C. Hayes, D. L. G. Hill, M. O. Leach, and D. J. Hawkes, "Non-rigid Registration Using Free-Form Deformations: Application to Breast MR Images." *IEEE Transactions on Medical Imaging*, 18(8), pp 712-721, 1999.
11. C. R. Meyer et al., "Demonstration of accuracy and clinical versatility of mutual information for automatic multimodality image fusion using affine and thin-plate" *Medical Image Analysis*, vol. 3, pp. 195-206, 1997
12. F. Maes, A. Collignon, and P. Suetens, "Multimodality image registration by maximization of mutual information," *IEEE Transaction on Medical Imaging* 16(2), pp. 187–198, April 1997.
13. J.D. Atkinson, D.L. Collins, G. Bertrand, T.M. Peters, G.B. Pike, and A.F. Sadikot, "Optimal location of thalamotomy lesions for tremor associated with Parkinson Disease: a probabilistic analysis based on postoperative magnetic resonance imaging and an integrated digital atlas*", J. Neurosurgery*, 96, pp. 854-866, 2002.